Electronic Journal of University of Aden for Basic and Applied Sciences
EJUA-BA Vol. 7 No. 1 (2026)
https://doi.org/10.47372/ejua-ba.2026.1.522
ISSN: 2708-0684

RESEARCH ARTICLE

# ADSORPTION OF METHYLENE BLUE ONTO YEMENI CAPPARIS SPINOSA LEAVES: KINETIC, ISOTHERM, AND THERMODYNAMIC MODELING STUDIES FOR SUSTAINABLE DYE REMEDIATION

**Abdul-Latif Abdullah Mahdi Saif[1,*], and Ahmed Awad Saleh Salah[2]**

[1] *Dept. of Chemistry, Faculty of Education, University of Aden, Yemen*
[1] *Dept. of Biology & Chemistry, Faculty of Toor Al-Baha University, University of Lahej, Yemen*

***Corresponding author: Ahmed Awad Saleh Salah; E-mail: aasalehsalah.74@gmail.com**

**Received: 13 March 2026 / Accepted: 30 March 2026 / Published online: 31 March 2026**

## Abstract

The release of dye contaminated effluents from industrial activities poses a serious threat to aquatic environments due to their toxicity, persistence, and aesthetic impact. In this study, dried leaves of *Capparis spinosa* (CPL) were evaluated as a low-cost and eco-friendly bio-adsorbent for the removal of methylene blue (MB) from aqueous solutions. Batch adsorption experiments were performed to investigate the effects of contact time, adsorbent dosage, initial dye concentration, solution pH, and temperature. Surface functional groups of CPL were identified using ATR-FTIR spectroscopy. Adsorption equilibrium, kinetic behavior, and thermodynamic feasibility were analyzed using Langmuir and Freundlich isotherms, pseudo-first-order and pseudo-second-order kinetic models, and thermodynamic parameters (ΔG°, ΔH°, ΔS°), respectively. The adsorption process were determined to be at pH 8, with the highest removal efficiency observed at pH 12. A contact time of 40 minutes and the removal attained to 91.58%, with an adsorption capacity of 1.99 mg/g. The highest adsorption capacity, 12.469 mg/g, was attained under conditions of 20 g/L dye concentration, 0.5 g dose and the optimum removal efficiency 99.95%. The equilibrium data were best fitted by the Langmuir model (R2=0.9997) fit than Freundlich model (R2=0.894), confirming a monolayer adsorption process on a homogeneous surface and the separation factor (RL) 0.4332 confirming that the adsorption of MB onto CPL is a favorable. While the kinetic data followed PSO model exhibited (R2= 0.9995) compared to the PFO model (R2=0.9296) and the calculated qe,cal (2.068 mg/g) close with the experimental qe,exp (1.99 mg/g). Thermodynamic analysis, where the positive enthalpy (ΔH°) 80.041kJ/mol confirmed that MB adsorption onto CPL is endothermic, and negative Gibbs free energy (ΔG°) values (-6.687, -9.597, -12.508, and -15.418kJ/mol) confirmed that the process is spontaneous. These results demonstrate that *Capparis spinosa* leaves are a promising sustainable adsorbent for dye-laden wastewater treatment.

**Keywords:** *Capparis spinosa*; Methylene blue; Bio-adsorbent; Equilibrium; Adsorption isotherms; Kinetics; Thermodynamics; Wastewater treatment.

## 1. Introduction

Water is the most vital natural resource, essential for both biological life and industrial applications. However, it is increasingly exposed to diverse pollutants stemming from human activities and industrial processes, rendering it unsuitable for reuse [1]. Major industries, including pulp and paper, tanneries, textiles, pharmaceuticals, and dye intermediates, are the primary consumers of synthetic dyes. It is estimated that 10–15% of the dyes used in these processes are discharged into natural water bodies or wastewater, representing a significant global environmental challenge [2,3]. Dyes are highly visible pollutants; even at low concentrations, they can severely impact aquatic life by reducing light penetration, which hinders photosynthesis. Furthermore, their anaerobic degradation can lead to the bioaccumulation of toxic amines. Consequently, the presence of color in wastewater poses a serious hazard to human health through the food chain and overall environmental stability. Moreover, several synthetic dyes exhibit mutagenic and carcinogenic properties [4,5]. Therefore, the removal of these organic pollutants is imperative. Various treatment methods have been developed, such as: chemical precipitation and electrochemical treatments. Aerobic/anaerobic microbial degradation and advanced oxidation processes. Membrane technologies

like ultrafiltration and reverse osmosis. Coagulation, flocculation, and adsorption eta [6,7]. While many of these techniques are complex, expensive, and require high technical expertise, the adsorption process stands out as one of the most effective methods. It is characterized by its ease of application, low cost, high efficiency, and minimal environmental impact. Adsorption also allows for the utilization of natural materials such as agricultural by-products, plant parts (leaves, flowers, fruits), cotton fiber, and biochar, which possess high specific surface areas and porous structures. These bioadsorbents contain critical functional groups, including phenolic, hydroxyl, and carboxyl groups, which facilitate the removal of organic pollutants from aquatic environments [8-12]. *Capparis spinosa* is an evergreen shrub belonging to the *Capparaceae* family, Fig.1 the picture of *Capparis spinosa*. It grows wild in rocky crevices, mud walls, and nutrient-poor soils. Its remarkable resistance to drought, salinity, and high temperatures has led to its wide distribution across the Canary Islands, Morocco, the Mediterranean, the Middle East, and as far as China [13, 14]. As an aromatic plant, Capparis is rich in carbohydrates, proteins, minerals, and vitamins (C, B1, B3, B6, B9, E, A, C, and K.), making it a valuable additive in the food industry. Furthermore, it is considered a medicinal herb; various parts of the plant (leave, flower, fruit, root, bark or whole and extracts) are used to treat diseases such as malaria, diabetes, and gastrointestinal infections, exhibiting anti-inflammatory, antioxidant, and antitumor activities. These properties are attributed to its bioactive functional groups, including glycosides, alkaloids, flavonoids, and phenolic acids [15-17]. Methylene Blue (MB), with the chemical formula $C_{16}H_{18}ClN_3S$, is a prominent cationic azo dye widely used in the pharmaceutical, textile, and cosmetic industries. Currently, MB is ranked among the most hazardous environmental pollutants, causing health issues such as eye burns, respiratory problems, and tissue necrosis. Its stable chemical structure makes it difficult to decompose, further impeding photosynthesis in aquatic ecosystems [18-20]. Based on the aforementioned literature, there is a lack of extensive research regarding the use of *Capparis spinosa* in adsorption processes. The Yemeni *Capparis spinosa* is natural abundance under various environmental condition, as previously indicated. Consequently, this study evaluates the efficiency of Capparis leaves as a bioadsorbent for removing Methylene Blue from aqueous solutions. The influence of parameters such as contact time, initial concentration, adsorbent dosage, and pH were investigated. Additionally, the data were analyzed using isotherm models (Langmuir and Freundlich) and kinetic models (Pseudo-first and Pseudo-second order), while The Attenuated Total Reflection-Fourier Infrared (ATR-FTIR) Spectroscopy was employed to identify the functional groups present on CPL that play major role in the adsorption process. Therefore, this work provides a scientific foundation for the utilization of CPL bio-sorbents as sustainable, economical, and environmentally friendly for industrial wastewater remediation.

**Fig. 1:** the picture of the Capparis spinosa plant


**Fig. 2:** Illustrated preparation of CPL absorbent

## 2. Experimental Methods

### *2.1. Materials:*

All chemicals including Methylene Blue (MB), hydrochloric acid (HCl), and sodium hydroxide (NaOH) were purchased from Merck (Germany) and used without further purification. Distilled water was used throughout the experiments. Furnace, Ball Mill: For grinding *Capparis spinosa* leaves, and digital pH-meter HQ411d–HACH for adjusted pH. The adsorbent and adsorbate solutions were mixed using an orbital shaker (Jlab Tech, Daihan Lab Tech Co. Ltd.) at 150 rpm. A centrifuge (model 80-1) and a single-beam UV-VIS spectrophotometer (LI-295) were used to measure MB concentrations at a wavelength of 664 nm. For functional group analysis, Attenuated Total Reflection-Fourier Transform Infrared spectroscopy (ATR-FTIR), PerkinElmer, USA) was employed.

### *2.2. Preparation Adsorbent CPL*

The adsorbent was prepared from *Capparis spinosa* leaves (CPL) collected from Abyan Governorate. The leaves were initially washed with distilled water to remove dust and surface impurities. For the drying process, the leaves were placed in a laboratory furnace at 70°C and maintained overnight to ensure complete dehydration. The leaves plant was pulverized using a mill to reduce the CPL's size obtain a fine and homogenous powder, the resulting material was filtered through a 125 µm mesh repeating this process several times. To ensure high purity, the resulting powder was re-washed with water and filtered to eliminate any leachable pigments or remaining impurities. After that, the filtered placed in a laboratory furnace at 70°C and maintained overnight. The final product of the CPL adsorbent was carefully stored in a vacuum desiccator to prevent moisture. Fig.2 illustrates the different stages of the preparation process.

### *2.3. Adsorbate Preparation:*

Methylene Blue (MB) powders the molecular weight 319.851 g/mole and chemical structure of the MB on Fig.3 [5]. Standard solution for adsorption studies prepared to the stock solution by weighed 1g and dissolved in 1 L of distilled water to get 1000 mg/L, from stock solution.

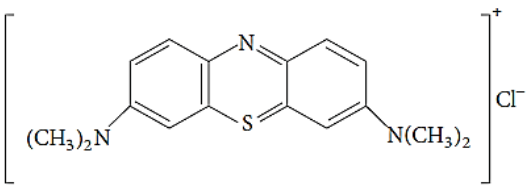


**Fig. 3:** Chemical structure of MB

### *2.4. Calibration of Methylene Blue:*

The synthetic dye sample calibrated in order to find out various optical densities at various concentrations was prepared using 5, 10, 15, 20, 25, and 30mg/L solution. The calibrated results are very effective to identify the respective color removal capacities of various adsorbents. Fig. 4 shown the graphical representation of Calibration of MB [21].

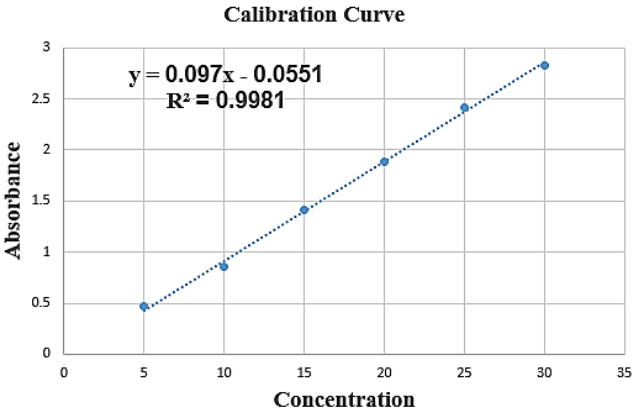


**Fig. 4:** Calibration of Methylene Blue.

### *2.5. Fourier Transform Infrared spectroscopy (FTIR)*

The Attenuated Total Reflection-Fourier Infrared (ATR-FTIR) Spectroscopy, that is rapid analysis and reliable results analytical technique and a one of the most applicable techniques in recent years in a different of disciplines such as forensic science, environmental, foods and industries etc, this analysis is perform with FTIR (PerkinElmer Spectrum Two) coupled with an ATR accessory equipped with a diamond crystal. Where a small amount of CPL powder analysis was directly place on the diamond crystal of the ATR accessory and measured in the region 4000–400 $cm^{-1}$, then, the instrument sends infrared light through the sample and measures absorption. The data is recorded and converted into a spectrum that shows the various peaks representing the functional groups in the sample, allowing for analysis based on their positions and intensities. [22-25]**.** the analysis in this study is focused on identifying of the functional groups in CPL.

### *2.6. Adsorption Procedure*

The Adsorption studies were performed for batch adsorption of MB solution onto CPL adsorbent surface to obtain rate and equilibrium data at different parameters such as pH (2-12), adsorbent dose (0.1-1.0 g), adsorbent concentration (5-50 mg/L), contact time (0-40 minutes) and temperature rang at 25, 35, 45 and 55°C. During the experiment, the pH of the solution was maintained by adding a small amount of 0.1M HCl or NaOH. The isotherm studies were employed by 50 mL of dye solution filled in 50 mL conical flasks. The agitation of samples were carried out by keeping in orbital shaker maintained it at constant temperature of 25°**C** under constant rpm of 150. After definite interval of time the aqueous samples were taken from solution and subjected to centrifugation at 4000 rpm for 15 min,

the results of the analysis of concentration samples were determined by monitoring the absorbance values for the most absorbance ($\lambda_{max}$; 664 nm) wavelength using a UV-vis spectrophotometer, reporting each data point as an average value of triplicates readings.

The equilibrium adsorption capacity of adsorbent (qt) and the percentage of dye removal were calculated using the equations 1 and 2 respectively [11]:

$$qe = \frac{V(Co-Ce)}{W} \quad (1)$$

$$\text{Removal Adsorption \%} = \frac{(Co-Ce)}{Co} 100 \quad (2)$$

Where: qe: the adsorbent capacity at equilibrium (mg/g), V: volume of the adsorbate (ml), $C_0$: dye concentration before adsorption (mg/L), C**e**: dye concentration after adsorption (mg/L), W: the weight in gram of the adsorbent (g).

## 3. Result and Discussion

### *3.1. The FTIR Analysis*

The ATR-FTIR spectra to identify function group of the CPL, these functional groups play a crucial role in surface interactions and adsorption processes [26] that shown in Fig.5, the broadband at 3287.85cm$^{-1}$ suggested the presence of O-H and N-H (amide) and may be due to the hydrogen bonding of phenols and alcohols [27]. The intense divided two peaks at 2920.8 and 2820.30 cm$^{-1}$ are probably related to stretching of C-H in methylene (-$CH_2$) and methyl (-$CH_3$) groups of alkanes, respectively. The A strong peak at 1634.15 cm$^{-1}$ attributed to amino acids with $NH_2$ groups [28, 29, 30], and it also, C=O carbonyl groups and the sp² C-C bond in aromatic ring [27]. The peak at 1548.5 cm$^{-1}$correspond to the bending vibration of N-H groups [14] and related to C=C stretching of aromatic ring deformations and to flavonoids [31]. The peaks represented by 1374.25 cm$^{-1}$ indicate the C-O-H [32], C-N stretching of amide [28] and could be related to bending vibrations of -$CH_2$ or-$CH_3$ groups in carboxylic acid and to C–O stretching of acid groups. The more intensity on the band at 1236.62 cm$^{-1}$ may be due to the stretching vibration of O–$CH_3$ and referred to bending vibration of O-H [31]. The strong band at 1049.65cm$^{-1}$ may be originated from the C-N [33] and attributed to C-O vibrations bonds functional groups present in aromatic or aliphatic that is associated with these oxygenated compounds (ketone, ether, alcohol, cellulose esters) [34] and may be referred to the stretching aromatic ring associated with CH in-plane bending. The peak a broad band at 518.84 cm$^{-1}$ assigned to the strong deformation of C-C-C and C-C-O [35] and may be referred to out-plane of -OH groups deformation mode of hydroxyl [36]. Finally, the spectra of observed in the range from 1370 to 518.84 cm$^{-1}$ and its functional groups mentioned above were indicating the predominance of phenolic oxygenated substances, flavonoids and tannins [37].

### *3.2. Effect of Contact Time.*

The influence of contact time on adsorption of MB onto CPL absorbent was investigated over a range of 0 to 40 min, using CPL amount 0.25 g/L and an initial dye concentration of 10 mg/L at room temperature. The results influence of contact time on adsorption of MB onto CPL absorbent was illustrated in Fig. 6, that is observed a rapid adsorption rate during the initial 15 min attained removal to 82.11%, reaching at equilibrium removal efficiency to 91.58%, this initial rapid phase can be attributed to the abundance of vacant active sites on the CPL surface and the strong affinity between MB molecules and the adsorbent. Subsequently, the adsorption rate significantly decreased, reaching 91.58% removal at 40 min, indicating that the system had approached equilibrium, this deceleration is likely maybe due to the gradual saturation of active sites as they become occupied by dye molecules, leading to a decline in adsorption efficiency over time. These observations are consistent with previous findings reported in the literature [12, 38, 39]. Consequently, a contact time of 40 min was selected for all further experiments.

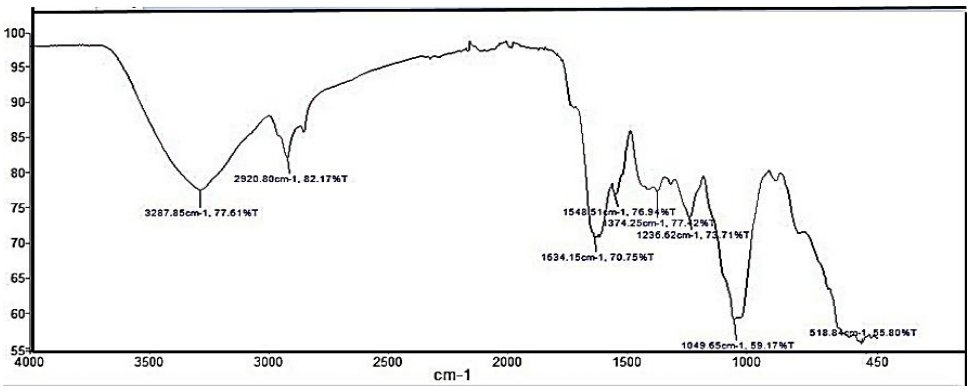


**Fig. 5:** FTIR of CPL

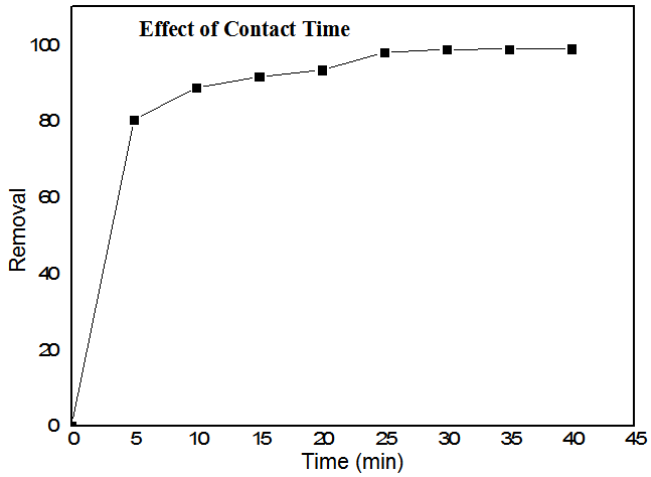


**Fig. 6:** The Effect of contact time.

### *3.3. Effect of Adsorbent Dosage on the Adsorption Process.*

The impact of adsorbent dosage on the removal of MB was investigated by varying the CPL amount from 0.1 to 1.0 g, using a 10 mg/L dye solution. As illustrated in Fig. 7 illustrated the impact of adsorbent dosage on the removal of MB, where the removal efficiency increased significantly with increase amount of CPL adsorbent, reaching at equilibrium (40min) 89.73 - 99.72% at amount of CPL adsorbent 0.1 - 0.5g. Moreover, the removal efficiency decreased with increase adsorbent dosages, where attained 98.97 - 93.82% for 0.75 - 1.0 g. This enhancement of adsorption is primarily attributed to the increased surface area and the higher number of available active sites onto CPL, which facilitate the transfer of MB molecules from the aqueous phase to the CPL adsorbent surface [4]. However, it was observed that the incremental increase in removal percentage becomes less significant at higher dosages, this phenomenon is often attributed to the aggregation of adsorbent particles, which leads to a decrease in the effective surface area and the overlapping of active sites [5, 9]. Based on these results, an adsorbent dosage of 0.5 g was selected as the optimum dose for subsequent experiments to ensure both high efficiency and cost-effectiveness.

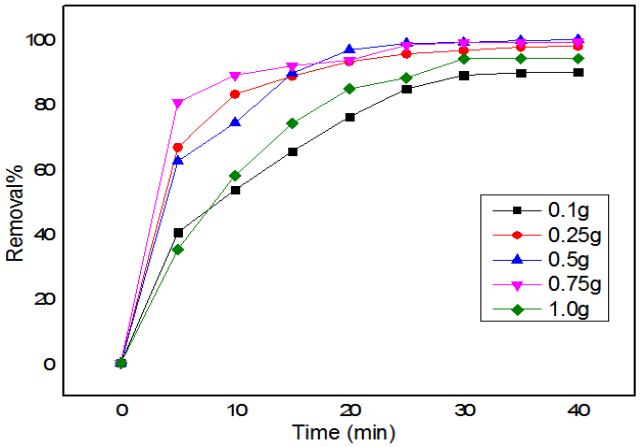


**Fig. 7:** The Effect of Adsorbent Dosage.

### *3.4. Effect of Initial Concentration*

The influence of initial MB concentration on adsorption efficiency was investigated across a range of 5 to 50 mg/L, using an adsorbent dosage of 0.5 g and a contact time of 40 min at room temperature. The influence of initial MB concentration on adsorption as shown in Fig. 8. Where the removal efficiency was highly dependent on the initial dye concentration. The highest removal rate reached from 97.43 to 57.89% for 5 to 50 mg/L, while at equilibrium (40 min) the removal efficiency of adsorption of the MB onto CPL attained 99.31, 99.58, 99.73, 91.11, 76.83, 61.81% at a concentration of 5, 10, 20, 30 40 and 50 mg/L respectively (Fig. 8). It was observed that the removal percentage was higher at lower initial concentrations, which can be attributed to the abundance of available active sites on the CPL surface relative to the number of MB molecules, thereby facilitating rapid mass transfer [19, 40]. Conversely, as the initial dye concentration increased, a gradual decline in removal efficiency was noted. This trend occurs because the active sites become increasingly saturated with dye molecules, leading to higher competition for the remaining vacant sites and a decrease in the overall adsorption performance. Similar observations regarding the relationship between initial concentration and removal percentage have been reported in previous studies [10, 41].

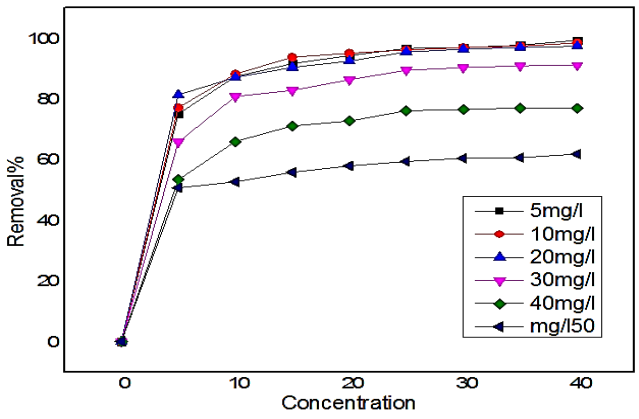


**Fig. 8:** Effect of Initial Concentration

### *3.5. Effect of pH*

The pH of the aqueous solution is a critical parameter in the adsorption process, as it influences the ionization state of the MB dye and the surface charge of the CPL adsorbent [34]. The adsorption performance was evaluated across a pH range of 2 to 12, using a 10 mg/L dye concentration and 0.5 g of adsorbent for 40 min. As illustrated in Fig. 9, the removal efficiency increased significantly with rising pH, reaching its maximum at pH 12. The percentage removal is increase with increase's pH 77.92, 82.42, 95.67, 99.79, 99.9, and 99.95% for at pH 2, 4, 6, 8, 10, and 12. There are two possibilities that the pH will affect the adsorption efficiency; The first possibility is the effect of pH on hydrogen ion ($H^+$), in

the acidic medium (low pH), the high concentration the H ions competes with the cationic MB molecules ($MB^+$) for the available active sites on the CPL surface, thereby reducing the adsorption capacity. As the pH increases toward alkaline conditions, the concentration of $H^+$ ions decreases, reducing this competition and facilitating higher dye uptake. Second possibility, the surface charge of the CPL is highly pH-dependent. In acidic conditions, the functional groups on the CPL adsorbent surface undergo protonation, creating a positive surface charge that leads to electrostatic repulsion with the cationic $MB^+$ molecules. Conversely, in alkaline media, deprotonation of these functional groups occurs, resulting in a negatively charged surface. This transition induces strong electrostatic attraction between the negative adsorbent surface and the positive MB+ ions, significantly enhancing the adsorption efficiency [34, 42]. These results demonstrate that CPL is a highly effective adsorbent for MB removal, particularly in neutral and alkaline environments.

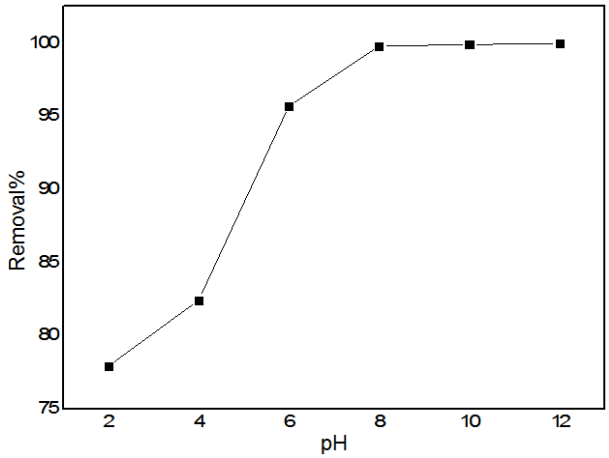


**Fig. 9:** Effect of pH

### *3.6. Effect of Temperature*

The effect of temperature on the adsorption of MB onto CPL was investigated at 25, 35, 45, and 55 °C, Fig.10 illustrates the influence of these temperatures on the removal rate and adsorption capacity. At the beginning of the process the removal efficiency increased significantly upon reaching equilibrium, the removal percentages were 99.42-99.97%, for the 25-55 °C temperatures. These results indicate that the adsorption process is enhanced by increasing temperature, confirming its endothermic nature. This positive temperature effect can be attributed to several factors. Firstly, increasing the temperature enhances the mobility of MB cations and reduces the solution viscosity [43], which increases the kinetic energy of the MB dye molecules and facilitates their diffusion across the boundary layer into the CPL adsorbent pores [44]. Secondly, higher temperatures may induce a "swelling effect" within the internal structure of the CPL adsorbent, enabling deeper spreading's of dye molecules into the active sites. Thirdly, elevated temperatures can activate additional functional groups on the adsorbent surface, strengthening the interaction between the CPL active sites and MB molecules [45, 46].

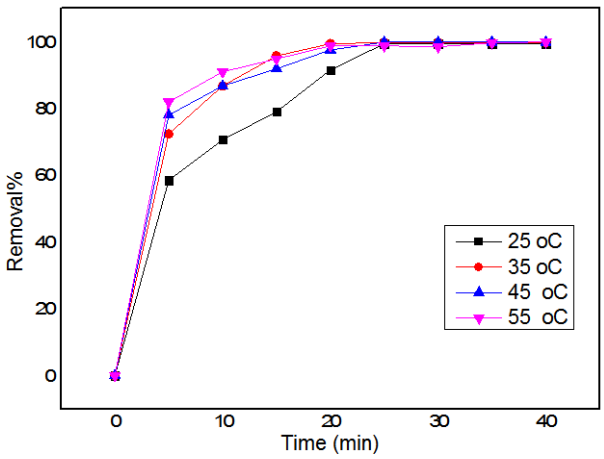


**Fig. 10:** The Effect of temperature on adsorption of CPL

### *3.7. Adsorption Thermodynamics*

The thermodynamic behavior of the adsorption process was evaluated using Gibbs free energy change (ΔG°), enthalpy change (ΔH°), and entropy change (ΔS°). The spontaneity of the adsorption is fundamentally dictated by the sign of ΔG°, where negative values signify a thermodynamically favorable and spontaneous process. Furthermore, the enthalpy change (ΔH°) distinguishes between endothermic and exothermic mechanisms, while the entropy change (ΔS°) reflects the variations in the degree of randomness at the solid-liquid interface during the adsorption [18].

The relationship between these parameters is defined by the following equations (3,4):

$$\Delta G° = -RT \ln Kc \qquad (3)$$

$$\Delta G° = \Delta H° - T\Delta S° \qquad (4)$$

The thermodynamic constants were derived from the Van't Hoff equation (5): [47]

$$ln\ Kc = \frac{\Delta S°}{R} - \frac{\Delta H°}{RT} \quad (5)$$

By constructing a linear plot of ln Kc versus 1/T, ΔH° and ΔS° were determined from the slope (-ΔH°/R) and the y-intercept (ΔS°/R), respectively, where R is the universal gas constant (8.314 J/mol·K) .

Fig 11 illustrates the adsorption thermodynamic study of MB onto CPL at various temperatures, and the thermodynamic parameters of MB adsorption on CPL showed in Table.1, the experimental results yielded a positive enthalpy change (ΔH°) of 80.041kJ/mol, confirming the endothermic nature of the adsorption process. The positive entropy value (ΔS° = 291.031J/mol·K°) suggests an increase in the

randomness at the adsorbent-solute interface during the sequestration of MB. Furthermore, the calculated ΔG° values were -6.687, -9.597, -12.508, and -15.418kJ/mol at 298, 308, 318, and 328 K°, respectively. The consistently negative values of ΔG° and their increase in magnitude with temperature indicate that the adsorption of MB onto CPL is spontaneous and more favorable with increased temperatures, this result is consistent with [38, 48, 49]. These findings underscore the high efficiency of CPL as a promising adsorbent for the remediation of MB from industrial wastewater.

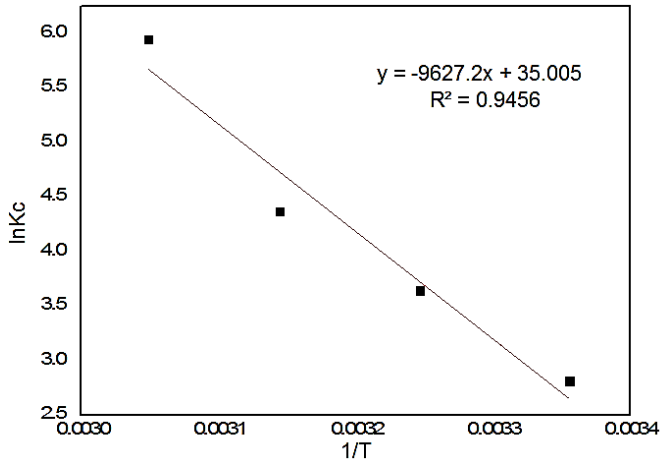


**Fig. 11:** Thermodynamic study of MB dye adsorption on CPL.

**Table 1:** Thermodynamic parameters of MB adsorption on CPL

| Intercept | Slope | ΔH(kJ/mol) | ΔS(J/mol/K | ΔG (kJ/mol) | | | |
|---|---|---|---|---|---|---|---|
| 35.005 | -9627.2 | 80.041 | 291.031 | 298 k° | 308 k° | 318 k° | 328 k° |
| y = -9627.2x + 35.005 | | | R² = 0.9456 | -6.687 | -9.597 | -12.508 | -15.418 |

### *3.8. Adsorption isotherms*

Adsorption isotherms are essential for understanding how MB molecules interact with the CPL surface and for determining the maximum adsorption capacity. In this study, the equilibrium data were analyzed using the two most common models: Langmuir and Freundlich.

#### *3.8.1. Langmuir Isotherm:*

This model assumes that adsorption occurs on a homogeneous surface with identical active sites and forms a monolayer.

The linear form of the Langmuir isotherm is given as (Eq. 6) [50]

$$\frac{Ce}{qe} = \frac{Ce}{q_{max}} + \frac{1}{KL\, q_{max}} \quad (6)$$

where: Ce (mg/L) is the equilibrium dye concentration, qe is the quantity (mg/g) of dye adsorbed at equilibrium, $q_m$ (mg/g) is the maximum monolayer capacity, and $K_L$ (L/mg) is the Langmuir constant. The values of $q_m$ and $K_L$ are obtained from the intercept and the slope of the linear plot of *Ce*/*q*e against *Ce* [50, 51].

To confirm the favorability of the adsorption process, the separation factor ($R_L$), was calculated by following equation 7:

$$Rl = \frac{1}{1 + KlCo} \quad (7)$$

Where; $C_o$ (mg/l) was initial dye concentration and $K_L$ (L/mg) is Langmuir constant.

According this factor the adsorption when: $R_L > 1$ is not favourable, $0 < R_L < 1$ is favourable, $R_L = 1$ considered the linear and $R_L = 0$ is irreversible adsorption [52].

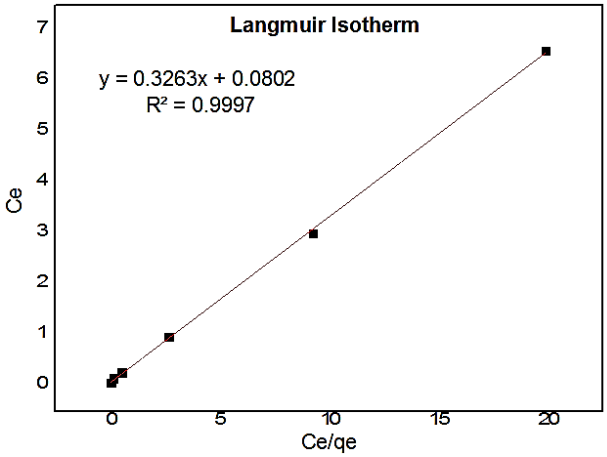


**Fig.12:** Langmuir′s isotherm models.

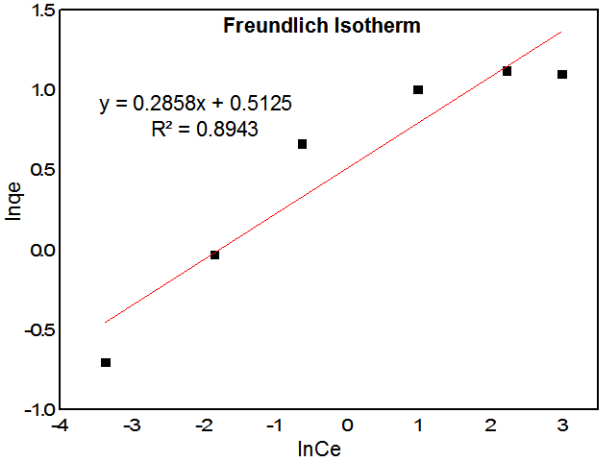


**Fig.13:** Freundlich′s isotherm models.

#### *3.8.2. Freundlich Isotherm:*

This model describes adsorption on a heterogeneous surface with multiple layers. Contrasted with Langmuir's theory, the Freundlich isotherm describes the heterogeneous adsorption of dye molecules at different sites with different surface energy. Therefore, the amount of dye adsorption changes with the exponential distribution of sites and adsorption energies.

The linear form of the Freundlich isotherm is given as (Eq. 8) [53].

$$log\ qe = logKf - \frac{1}{n}\ \text{logCe} \qquad (8)$$

where $K_f$ and n are Freundlich constants representing adsorption capacity(mg/g).(L/mg) and intensity, respectively.

The values of n and $K_f$ can be computed from are obtained from the slope and intercept of the linear plot of $\log q_e$ and $\log C_e$.

In addition, if the value of Freundlich' heterogeneity factor (n) between 2 and 4 is a favorable adsorption [20][54].

**Table 2:** Parameters of Langmuir and Freundlich equations for sorption of MB onto CPL

| Freundlich | | Langmuir | |
|---|---|---|---|
| Slope | 0.2858 | Slope | 0.3263 |
| Intercept | 0.5125 | Intercept | 0.0802 |
| $k_f$ | 1.669 | $q_{max}$ | 12.469 |
| n | 3.499 | $K_L$ | 0.0262 |
| $R^2$ | 0.894 | $R^2$ | 0.9997 |
| y = 0.2858x + 0.5125 | | $R_L$ | 0.4332 |
| | | y = 0.3263x + 0.0802 | |

The experimental data for the MB removal were tested with Langmuir and Freundlich isotherms were elucidated in the Fig.12, 13 and in Table 2. By comparing the correlation coefficients ($R^2$), it was found that the Langmuir model provided a better fit ($R^2$ 0.9997) than the Freundlich model ($R^2$ 0.894), that is indicates the formation of monolayer coverage at the outer a homogeneous surface of the adsorbent with no interactions occurring between MB molecules and adjacent sites [isotherm [55, 56]. It is also the values of $q_m$ 12.469 mg/g and $K_L$ 0.0262 L/mg showing high adsorption energy and contributing to the fast increment in adsorption and various MB concentrations. [57, 58]. Moreover, the separation factor ($R_L$) was 0.4332, this values confirming that the adsorption of MB onto CPL is a favorable, this results agreement with [59, 60].

### *3.9. Kinetics study:*

Adsorption kinetics is a fundamental aspect of environmental engineering, explaining the interaction between adsorbate molecules and the adsorbent surface over time. This process encompasses complex phenomena such as diffusion, mass transfer, and the progressive saturation of the adsorbent surface [61]. Generally, adsorption capacity increases rapidly in the early stages due to the high availability of adsorption sites, eventually slowing down as the surface becomes almost completely covered by MB molecules until equilibrium is reached [62].

Investigated in this study by two models Pseudo First-Order (PFO) and Pseudo-Second-Order (PSO) that is widely utilized for describing surface reactions adsorption. The PFO model assumes that the rate at which adsorption sites are occupied is directly related to the number of available sites. This model often demonstrates a two-stage kinetic behavior: an early phase of rapid reaction followed by a slower subsequent phase. This pattern suggests a process taking place initially in readily accessible regions and later in less accessible interior regions. The PFO model is particularly suitable for systems where the adsorption follows a simple molecular exchange pattern, where the rate is linearly related to the concentration of adsorbed molecules [63, 64].

The PFO kinetics can be expressed as linearized formula by using follows equation 9:

$$\log(qe - qt) = logqe - \frac{\text{K1}}{2.303}\text{t} \qquad (9)$$

where, $q_e$ (mg/g), $q_t$ (mg/g) and $k_1$ (1/min) are the adsorption amounts at equilibrium, a given time (t), and the rate constants, respectively. The graphical plots of $log\ (q_e - q_t)$ against t yielded a straight line consequently can be calculate the value of t rate constants $k_1$ from slope and $q_e$ value from intercept.

The PSO model is predicated on the premise that the rate-limiting step involves chemical adsorption (chemisorption) facilitated by valence forces, involving the sharing or exchange of electrons. Unlike the PFO model, the PSO model assumes the adsorption rate depends on the square of the number of free sites [38, 63]. In many investigations, the PSO model has demonstrated superior correlation with experimental data, with correlation coefficients ($R^2$) very close to 1 [65]. Furthermore, the proximity between calculated and experimental equilibrium capacity (qe) values often confirms that the PSO model is the most appropriate choice for explaining the adsorption of dyes [61].

The linear equation 10. representation of the PSO kinetics:

$$\frac{\text{t}}{q_t} = \frac{1}{K_2 q_e^2} + \frac{1}{q_e}\text{t} \qquad (10)$$

where, $q_e$ (mg/g), $q_t$ (mg/g) and $k_2$ (g/mg mint) are the adsorption amounts at equilibrium, a given time (t), and the rate constants, respectively. Plotting the quantity of $t/q_t$ against t at varying initial concentrations yielded a straight line consequently, can be calculate the values of $q_e$ from slope and $k_2$ from intercept.

Fig.14 and 15 illustrated the kinetic results and from the calculated parameters for adsorption kinetics data that reported in the table.3. Based on the results, the PSO model exhibited a higher correlation coefficient ($R^2$ = 0.9995) compared to the PFO model **(**$R^2$ = 0.9296**)**. Furthermore, the calculated $q_{e,cal}$ values (2.068 mg/g) from the PSO model were in close agreement with the

experimental $q_{e,exp}$ values (1.99 mg/g). The PSO indicate to physisorption process with involve chemisorption process due to a strong affinity interaction between of surface CPL and MB, this chemical adsorption processes take place by valence forces and exchange electrons**,** with physisorption is the step rate limiting of adsorption, this result finding [12, 7, 66].

**Table 3:** Adsorption kinetics parameters of pseudo-first-order rate and pseudo-second-order

| Pseudo First Order | | Pseudo Second Order | |
|---|---|---|---|
| slope | -0.19205 | slope | 0.4835 |
| intercept | 0.58976 | intercept | 0.8064 |
| $R^2$ | 0.9298 | $R^2$ | 0.9995 |
| $K_1$ | 0.192 $min^{-1}$ | $q_{cal}$ | 2.068 mg/g |
| $q_e$ | 1.804 mg/g | $k_2$ | 0.599 g/mg min |
| y = -0.19205x + 0.58976 | | y = 0.4835x + 0.8064 | |
| qe experimental | 1.99 mg/g | | |

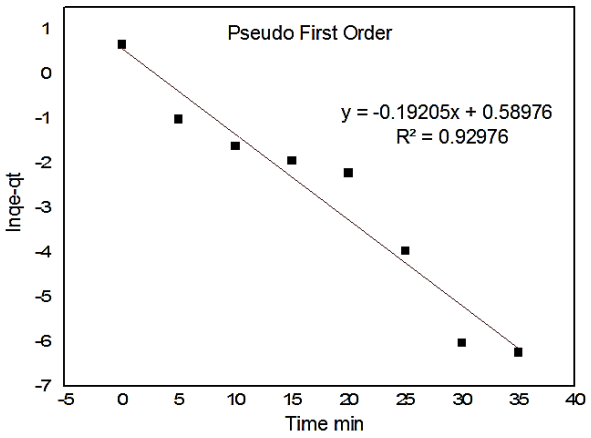


**Fig.14:** Pseudo first order kinetic models.

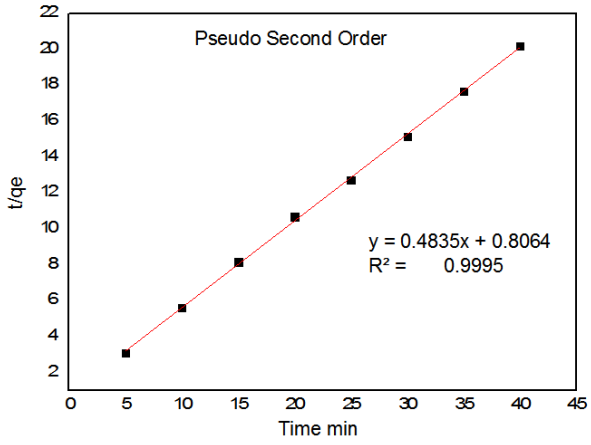


**Fig.15:** pseudo second order kinetic models.

### *3.10. The Adsorption Mechanism*

### *Adsorption Mechanism of Methylene Blue onto Capparis spinosa Leaves Powder (CPL)*

The adsorption mechanism of methylene blue (MB) onto Capparis spinosa leaves powder (CPL), which containing; alkaloids, flavonoids, glycosides, tannins, , phenolic, proteins, cellulose, hemicellulose, lignin and other components, that are containing functional groups including C=O, COOH, –OH, –NH, NHR and aromatic ring. The FTIR spectra confirmed that the CPL surface has abundance of polar with in numerous active sites on surface. The PSO suggests that the adsorption rate is controlled by formed a strong adsorbate–adsorbent interactions between MB and CPL and may involve both physisorption and chemisorption contributions. This interaction occur on a monolayer, a homogeneous CPL surface with energy equivalent active sites, reaching equilibrium upon full site occupation, which is proven by Langmuir isotherm experimental and the thermodynamically, suggests that the adsorption process is spontaneous and endothermic, as demonstrated by the negative free energy Gibes (ΔG°) and positive enthalpy change (ΔH°). This gives the possibility of several to understanding the adsorption mechanisms;

**Electrostatic Attraction:** functional groups such as –COOH and –OH given a negative polarity of the surface on the CPL exhibited strong electrostatic attraction between the negatively charged surface sites and the cationic methylene blue molecules ($MB^+$).

**Ion Exchange Mechanism:** Ion exchange also contributes to the adsorption process. at alkaline pH, enable to ion exchange interaction due to the deprotonation of acidic functional groups (ionized) may be replacing $H^+$ or other ions on the surface CPL with ions $MB^+$ from the aqueous solution. The increase in removal efficiency at alkaline pH strongly supports the contribution of electrostatic interactions. **Hydrogen Bonding:** Hydrogen bonding interactions can occur, due to the structure of MB containing S and N atoms rich electron-pair leads to formation of a hydrogen bond with hydrogen groups on the CPL surface (–OH and –NH groups) of active sites on surface of CPL make the increased adsorption capacity. ***π–π* Interactions:** Methylene blue contains aromatic rings with delocalized π-electrons. These rings can interact with aromatic or conjugated structures present in the carbonaceous matrix of CPL through π–π stacking interactions between them. This type of interaction enhances adsorption, particularly when the adsorbent contains lignocellulosic components with aromatic moieties, similar mechanisms have been widely reported by [7, 19, 42, 67, 68].

The adsorption mechanisms of methylene blue onto CPL are driven by a combination of different interactions as shown in Fig. 16 and the adsorption of MB onto CPL on Fig.17. In the end, we suggested the our results make CPL adsorbents high performance to remove MB, a very high performance, to be simple, sustainable, abundant, and cheap.

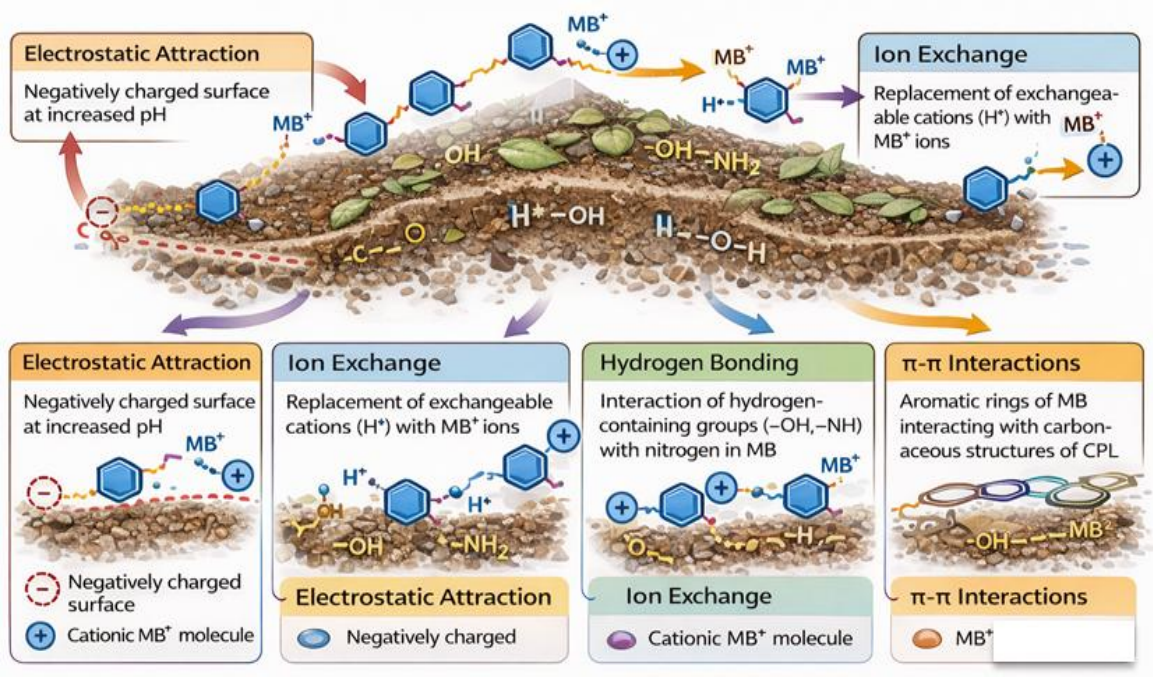


**Fig.16:** Possible adsorption mechanisms of MB onto CPL: electrostatic attraction, Ion Exchange, Hydrogen Bonding, and π-π interaction, respectivily.

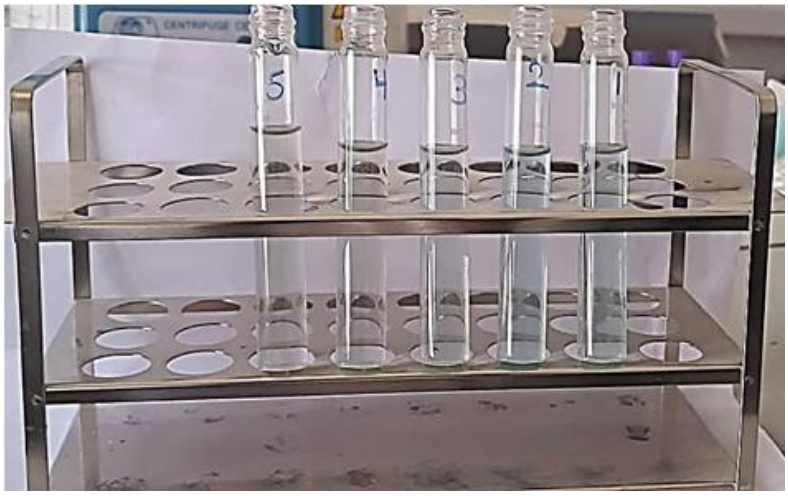


**Fig.17:** adsorption of MB onto CPL

## 4. Conclusions

The present study successfully demonstrated the feasibility of using Capparis spinosa leaves (CPL) as a sustainable and low-cost adsorbent for Methylene Blue (MB) removal from aqueous solutions. The simple preparation method (oven-drying at 70°C) proved effective in maintaining the adsorbent's functional efficiency without the need for high-energy carbonization processes. The ATR-FTIR analysis revealed the presence of functional groups such as –OH, –COOH, –NH, and –NHR on the surface of CPL. These groups provide multiple active sites that facilitate the adsorption of MB molecules. The study introduced a simple preparation method (drying CPL at 70°C) proved effective in maintaining the adsorbent's functional efficiency without the need for high-energy carbonization processes. The optimal conditions of these results demonstrate that CPL is a highly effective adsorbent for MB removal reached equilibrium within a short contact time of 40 minute and the removal attained to 91.58%, with an adsorption capacity of 1.99 mg/g. The highest adsorption capacity, 12.469 mg/g, was attained under conditions of 20 g/L dye concentration, 0.5 g dose and the optimum removal efficiency 99.95%. It is also the CPL showed multiple efficiency in adsorption of MB dye at pH 8, with the highest removal efficiency observed at pH 12. The CPL showed multiple efficiency in adsorption of MB dye at multiple pH and It is also CPL showed multiple efficiency in adsorption of MB dye at temperature.

Kinetic studies revealed, the PSO model exhibited ($R^2$ = 0.9995) compared to the PFO model **(**$R^2$ = 0.9296**)** and the calculated $q_{e,cal}$ (2.068 mg/g) close with the experimental $q_{e,exp}$ (1.99 mg/g). The PSO indicate indicating that chemical interactions play a dominant role in dye sequestration. Based on the results of the equilibrium data were best described by the Langmuir isotherm ($R^2$ = 0.9997) than Freundlich model ($R^2$ 0.894), confirming a monolayer adsorption process on a homogeneous surface with a high affinity between MB and CPL. It is also the values of $q_m$ 12.469 mg/g and $K_L$ 0.0262 L/mg showing high adsorption energy and the separation factor ($R_L$) was 0.4332, this values confirming that the adsorption of MB onto CPL is a favorable. Moreover the CPL has thermodynamic nature, where the results reviled the positive enthalpy (ΔH°)80.041kJ/mol confirmed that the process is endothermic, and negative Gibbs free energy (ΔG°) values (-6.687, -9.597, -12.508, and -15.418kJ/mol) confirmed that the process is and spontaneous, with increased efficiency at higher temperatures and the positive entropy value (ΔS°=291.031J/mol·K°) suggests an increase in the randomness at the adsorbent-solute interface during the uptake of MB. Overall, these findings underscore the high efficiency of CPL as a promising adsorbent for the remediation of MB from industrial wastewater.

## 5. Recommendations

This study addresses the critical issue of industrial dye pollution by evaluating the leaves of *Capparis spinosa* (CPL), a plant native to Yemen, as a sustainable bio-adsorbent for Methylene Blue (MB). The use of locally available, low-cost materials for wastewater treatment is of significant environmental and economic importance.

Based on the promising results obtained in this study, the following recommendations are suggested for future research:

- Future studies could explore using of CPL to its adsorption capacity and selectivity for different types of pollutants.
- It is recommended to application CPL on to real wastewater (from textile or leather industries, etc.), as real wastewater contains a mixture of dyes, salts and minerals that may affect pollution water.
- It is recommended to investigate the competitive adsorption of MB in the presence of other dyes or heavy metal ions to understand the interference effects in complex systems.
- It is recommended to perform TEM, SEM, and BET analyses on the CPL to gain deeper insights into the structural changes and the specific binding sites involved.

## Acknowledgements

The authors gratefully acknowledge the Dr. Khalid Saeed Al-Suwaidi for the laboratory access of the Faculty of Pharmacy, University of Aden.

Funding there is no funding for this article.

## Ethics approval and consent to participate

Not applicable.

## Declarations

Conflict of interest the authors declare that they have no known competing financial interests or personal relationships that could have appeared to influence the work reported in this paper.

The authors acknowledge the use of generative AI-based tools specifically for the graphical enhancement of figure 2 and 16.

## References

[1] D. Jaspal, A. Malviya, I. Tyagi, S. Khamparia, and V. Gupta, "Decolorization of mixture of dyes: A critical review," Global J. Environ. Sci. Manage., vol. 1, no. 1, pp. 71-94, 2015. https://doi.org/10.7831/gjesm.2015.01.01.007.

[2] Z. Carmen and S. Daniela, "Textile organic dyes-characteristics, polluting effects and separation/elimination procedures from industrial effluents-a critical overview," Journal of Engineering and Science, vol. 3, pp. 55–86, 2012. https://doi.org/10.5772/32373

[3] D. S. Kharat, "Preparing agricultural residue based adsorbents for removal of dyes from effluents-a review," Brazilian J. Chem. Eng., vol. 32, no. 1, pp. 1-12, 2015. https://doi.org/10.1590/0104-6632.20150321s00002991

[4] S. Bhattacharjee, "Adsorptive removal of methylene blue using Azadirachta indica (neem) leaf," Int. Res. J. Environ. Sci., vol. 5, no. 1, pp. 21-24, 2016.

[5] Ö. Dülger, F. Turak, K. Turhan, and M. Özgür, "Sumac leaves as a novel low-cost adsorbent for removal of basic dye from aqueous solution," Int. Sch. Res. Notices, vol. 2013, art. no. 210470, 2013. https://doi.org/10.1155/2013/210470

[6] L. Bulgariu, L. B. Escudero, O. S. Bello, M. Iqbal, J. Nisar, K. A. Adegoke, and I. Anastopoulos, "The utilization of leaf-based adsorbents for dyes removal: A review," J. Mol. Liq., vol. 276, pp. 728-747, 2019. https://doi.org/10.1016/j.molliq.2018.12.001

[7] A. Yildirim and H. Acay, "Methylene blue and malachite green dyes adsorption onto Russula delica/bentonite/tripolyphosphate," Heliyon, vol. 11, no. 1, 2025. https://doi.org/10.1016/j.heliyon.2024.e41984

[8] P. Velmurugan, V. Rathinakumar, and G. Dhinakaran, "Dye removal from aqueous solution using low cost adsorbent," Int. J. Environ. Sci., vol. 1, no. 7, pp. 1492-1503, 2011.

[9] M. B. Ibrahim and S. Sani, "Neem (Azadirachta indica) leaves for removal of organic pollutants," J. Geosci. Environ. Prot., vol. 3, no. 2, pp. 1-9, 2015. https://doi.org/10.4236/gep.2015.32001

[10] S. Gupta, A. Prajapati, and A. Kumar, "Removal of anionic dyes by magnetic modified A. barbadensis Miller residue leaves as a bio-adsorbent using biosorption process," Green Technol. Sustain., vol. 3, no. 3, art. no. 100196, 2025.

[11] M. Kurniasih, N. H. Aprilita, R. Roto, and M. Mudasir, "Modification of coal fly ash for high capacity adsorption of methylene blue," Case Stud. Chem. Environ. Eng., vol. 11, art. no. 101101, 2025. https://doi.org/10.1016/j.cscee.2024.101101

[12] M. M. Gaber, S. H. Hassanin, A. H. Awad, S. M. Samy, and Elkady. M, "Novel palm peat lignocellulosic adsorbent derived from agricultural residues for efficient methylene blue dye removal from textile wastewater," Appl. Water Sci., vol. 15, no. 2, art. no. 32, 2025.

[13] M. Rajabi, M. R. Azimi Moghadam, A. Azizi, and J. Soltani, "Isolation and molecular identification of two rutin-producing endophytic fungi from Caper (Capparis spinosa L.)," J. Microb. Biol., vol. 11, no. 44, pp. 169-180, 2022. https://doi.org/10.30495/jmb.2022.691238

[14] F. Benakashani, A. R. Allafchian, and S. A. H. Jalali, "Biosynthesis of silver nanoparticles using Capparis spinosa L. leaf extract and their antibacterial activity," Karbala Int. J. Mod. Sci., vol. 2, no. 4, pp. 251-258, 2016. https://doi.org/10.1016/j.kijoms.2016.08.002

[15] N. Benzidane, R. Aichour, S. Guettaf, N. Laadel, S. Khennouf, A. Baghiani, and L. Arrar, "Chemical investigation, the antibacterial and antifungal activity of different parts of Capparis spinosa extracts," J. Drug Deliv. Ther., vol. 10, no. 5, pp. 118-125, 2020. https://doi.org/10.22270/jddt.v10i5.4382.

[16] S. Chedraoui, A. Abi-Rizk, M. El-Beyrouthy, L. Chalak, N. Ouaini, and L. Rajjou, "Capparis spinosa L. in a systematic review: A xerophilous species of multi values and promising potentialities for agrosystems under the threat of global warming," Front. Plant Sci., vol. 8, art. no. 1845, 2017. https://doi.org/10.3389/fpls.2017.01845

[17] H. Annaz, Y. Sane, G. T. M. Bitchagno, W. Ben Bakrim, B. Drissi, I. Mahdi, and M. Sobeh,"Caper (Capparis spinosa L.): an updated review on its phytochemistry, nutritional value, traditional uses, and therapeutic potential," Front. Pharmacol., vol. 13, art. no. 878749, 2022. https://doi.org/10.3389/fphar.2022.878749

[18] S. Kumari, A. Verma, P. Sharma, S. Agarwal, V. D. Rajput,T. Minkina, and M. C. Garg, "Introducing machine learning model to response surface methodology for biosorption of methylene blue dye using Triticum aestivum biomass," Sci. Rep., vol. 13, no. 1, art. no. 8574, 2023. https://doi.org/10.1038/s41598-023-35326-y

[19] B. Belahrach, M. Farah, N. Samghouli, N. Gadda, M. Bensemlali, N. Labjar, and S. E. Hajjaji, "Investigation of equilibrium and kinetic aspects of methylene blue dye adsorption from aqueous solutions using raw and extract of Eriobotrya japonica seeds," Euro-Mediterr. J. Environ. Integr., pp. 1-15, 2025. https://doi.org/10.1007/s41207-024-

[20] N. L. Bih, M. J. Rwiza, A. S. Ripanda, A. A. Mahamat, R. L. Machunda, and J. W. Choi, "Adsorption of phenol and methylene blue contaminants onto high-performance catalytic activated carbon from biomass residues," Heliyon, vol. 11, no. 1, 2025. https://doi.org/10.1016/j.heliyon.2024.e41575.

[21] P. Velmurugan, V. Rathinakumar, and G. Dhinakaran, "Dye removal from aqueous solution using low cost adsorbent," Int. J. Environ. Sci., vol. 1, no. 7, pp. 1492-1503, 2011.

[22] I. Chrisikou, M. Orkoula, and C. Kontoyannis, "FT-IR/ATR Solid Film Formation: Qualitative and Quantitative Analysis of a Piperacillin-Tazobactam Formulation," Molecules, vol. 25, art. no. 6051, 2020. https://doi.org/10.3390/molecules25246051

[23] S. Kwon, S. Lee, J. Jang, B. J. Lee, and S. K. Kim, "Quantifying the effects of repeated dyeing: Morphological, mechanical, and chemical changes in human hair fibers," Heliyon, vol. 10, art. no. e37871, 2024. https://doi.org/10.1016/j.heliyon.2024.e37871

[24] P. Fermo, L. Andrea, C. D. Alfonsina, G. Vittoria, G. Benedetta, T. Alice, P. Massimiliana, C. Valeria, B. Andrea, G. Lorenzo and P. Patrizia, "Disclosing Colors and Pigments on Archaeological Objects from the Aga Khan Necropolis (West Aswan Egypt) through On-Site Analytical Methods: Preliminary Results," Heritage, vol. 7, pp. 4980-4996, 2024. https://doi.org/10.3390/heritage7090234.

[25] A. Bartošová, L. Blinová, M. Sirotiak, and A. Michalíková, "Usage of FTIR-ATR as Non-Destructive Analysis of Selected Toxic Dyes," Res. Pap. Fac. Mater. Sci. Technol. Slovak Univ. Technol., vol. 25, no. 40, pp. 39-47, 2017. https://doi.org/10.1515/rput-2017-0005

[26] M. Moheb, A. M. El-Wakil, and F. S. Awad, "Highly porous activated carbon derived from the papaya plant (stems and leaves) for superior adsorption of alizarin red s and methylene blue dyes from wastewater," RSC Adv., vol. 15, no. 1, pp. 674-687, 2025. https://doi.org/10.1039/D4RA08226A

[27] K. A. Hreeba, A. E. Khalil, and M. H. Awad, "Green Synthesis of Silver Nanoparticles Using Capparis Spinosa L.(Qapar) Leaf from Libya and Their Characterization Using XRD Technology," Afr. Asian J. Sci. Res. (AAJSR), pp. 199-207, 2025.

[28] H. A. Murthy, T. Desalegn, M. Kassa, B. Abebe, and T. Assefa, "Synthesis of green copper nanoparticles using medicinal plant Hagenia abyssinica (Brace) JF. Gmel. leaf extract: Antimicrobial properties," J. Nanomater., vol. 2020, art. no. 3924081, 2020. https://doi.org/10.1155/2020/3924081

[29] F. M. Abdoon, H. M. Hasan, S. A. Salman, S. T. Ameen, and M. Birhan, "Exploiting of green synthesized silver nanoparticles using Capparis spinosa L. Fruit for spectrophotometric determination of diphenhydramine HCl in pure forms and commercial products," J. Exp. Nanosci., vol. 18, no. 1, art. no. 2161525, 2023. https://doi.org/10.1080/17458080.2023.2161525

[30] K. Ebrahimi, M. Madani, B. Ashrafi, S. Shiravand, and A. Sepahvand, "Antifungal Properties of Silver Nanoparticles Synthesized From Capparis Spinosa Fruit," Res. Mol. Med., vol. 7, no. 4, pp. 43-50, 2019. https://doi.org/10.32598/rmm.7.4.43

[31] R. N. Oliveira, M. C. Mancini, F. C. S. D. Oliveira, T. M. Passos, , B. Quilty, R. M. D. Thiré and G. B. McGuinness, "FTIR analysis and quantification of phenols and flavonoids of five commercially available plants extracts used in wound healing," Matéria (Rio de Janeiro), vol. 21, no. 3, pp. 767-779, 2016. https://doi.org/10.1590/S1517-707620160003.0073

[32] S. A. Neamah, S. Albukhaty, I. Q. Falih, Y. H. Dewir, and H. B. Mahood, "Biosynthesis of zinc oxide nanoparticles using Capparis spinosa L. fruit extract: characterization, biocompatibility, and antioxidant activity," Appl. Sci., vol. 13, no. 11, art. no. 6604, 2023. https://doi.org/10.3390/app13116604

[33] M. K. Daish, M. A. Muhammad-Ali, and W. M. T. Al-Asadi, "Green Synthesis of Nanoparticles Using Aqueous Leaves Extract of Capparis spinosa L. and Evaluation of their Resistance to Salt Stress of some Aquatic Plants," IOP Conf. Ser.: Earth Environ. Sci., vol. 1371, no. 2, art. no. 022003, 2024. https://doi.org/10.1088/1755-1315/1371/2/022003.

[34] M. Benjelloun, Y. Miyah, S. Ssouni, S. Iaich, M. El-habacha, S. Lagdali, and R. Bouslamti, "Capparis spinosa L waste activated carbon as an efficient adsorbent for crystal violet toxic dye removal: Modeling, optimization by experimental design, and ecological analysis," Chin. J. Chem. Eng., vol. 71, pp. 283-302, 2024. https://doi.org/10.1016/j.cjche.2024.03.023

[35] L. Hssaini, R. Razouk, and Y. Bouslihim, "Rapid prediction of fig phenolic acids and flavonoids using mid-infrared spectroscopy combined with partial least square regression," Front. Plant Sci., vol. 13, art. no. 782159, 2022. https://doi.org/10.3389/fpls.2022.782159

[36] M. A. Elbager, H. A. Asmaly, M. Al-Suwaiyan, A. I. Ibrahim, and H. Dafallah, "High Performance Batch Adsorption of Methylene Blue Using Desert Date Seed Shell Activated Carbon: Characterization and Response Surface Methodology Optimization," Water, Air, & Soil Pollut., vol. 236, no. 4, art. no. 233, 2025. https://doi.org/10.1007/s11270-025-07851-4

[37] I. Rajhi, F. Hernandez-Ramos, M. Abderrabba, M. T. Ben Dhia, S. Ayadi, and J. Labidi, "Antioxidant, Antifungal and Phytochemical Investigations of Capparis spinosa L.," Agriculture, vol. 11, no. 10, art. no. 1025, 2021. https://doi.org/10.3390/agriculture11101025.

[38] M. A. Woldehana, M. A. Hiruy, and A. T. Feseha, "Removal of Methylene Blue from Aqueous Solutions Using Rumex Nepalensis Leaf and Roots as a Low-cost Adsorbents: Isotherm, Kinetics, and Thermodynamic Studies," Appl. J. Environ. Eng. Sci., vol. 11, no. 1, pp. 63-73, 2025.

[39] S. Yetgin and M. Amlani, "Agricultural low-cost waste adsorption of methylene blue and modelling linear isotherm method versus nonlinear prediction," Clean Technol. Environ. Policy, vol. 27, pp. 1205-1225, 2025. https://doi.org/10.1007/s10098-024-03023-3

[40] T. K. Sen, "Adsorptive Removal of Dye (Methylene Blue) Organic Pollutant from Water by Pine Tree Leaf Biomass Adsorbent," Processes, vol. 11, no. 7, art. no. 1877, 2023. https://doi.org/10.3390/pr11071877

[41] J. Y. Liu, E. Li, X. J. You, C. W. Hu, and Q. G. Huang, "Adsorption of methylene blue on an agro-waste oiltea shell with and without fungal treatment," Sci. Rep., vol. 6, no. 1, pp. 1-9, 2016. https://doi.org/10.1038/srep21458

[42] M. A. Hassaan, M. Yılmaz, M. Helal, M. A. El-NemrS. , Ragab and A. El Nemr, "Improved methylene blue adsorption from an aqueous medium by ozone-triethylenetetramine modification of sawdust-based biochar," Sci. Rep., vol. 13, no. 1, art. no. 12431, 2023. https://doi.org/10.1038/s41598-023-39446-z

[43] H. A. Al-Aoh, M. H. Meshari, A. A. Aljohania, M. Darwish, A. Ayaz, S. A. Bani-Attaa, A. Meshari, Y. M. Alsharifa, H.S, L. R. Al-Shehrig and J. N. A. "A potentially low-cost adsorbent for methylene blue removal from synthetic wastewater," Desalin. Water Treat., vol. 213, pp. 431–440, 2021. https://doi.org/10.1038/s41598-023-39495-7

[44] N. Sivarajasekar, R. Baskar, T. Ragu,. K. Sarika, N. Preethi and T. Radhika "Biosorption studies on waste cotton seed for cationic dyes sequestration: equilibrium and thermodynamics," Appl. Water Sci., vol. 7, pp. 1987-1995, 2017. https://doi.org/10.1007/s13201-016-0378-3

[45] P. D. Egwuonwu, "Adsorption of Methyl Red and Methyl Orange Using Different Tree Bark Powder," Acad. Res. Int., vol. 4, no. 1, pp. 330-338, 2013.

[46] H. Tahir, U. Hammed, Q. Jahanzeb, and M. Sultan, "Removal of fast green dye (C.I. 42053) from an aqueous solution using Azadirachta indica leaf powder as a low cost adsorbent," Afr. J. Biotechnol., vol. 7, no. 21, pp. 3906-3911, 2008 https://doi.org/10.5897/AJB08.681.

[47] K. A. Raj, "Adsorption of Methylene Blue Dye from Textile Industry Effluent using Activated Carbon Synthesized from Various Plant-Based Precursors," Orient. J. Chem., vol. 41, no. 2, pp. 665-674, 2025. https://doi.org/10.13005/ojc/410228.

[48] K. R. Adday and M. H. Flayeh, "Removal of Methylene Blue from Wastewater Using AL Haji Plant as a Low-Cost, Eco Friendly Adsorbent," Al-Khwarizmi Eng. J., vol. 21, no. 2, pp. 23-41, 2025. https://doi.org/10.22153/kej.2025.02.001

[49] I. N. Taib, R. Saleh, A. A. Fisol, I. I. Ismail and N. N. Ismail, "Adsorptive removal of methylene blue using magnetic graphitic carbon nitride (Fe3O4/g-C3N4) composite: insights into isotherms, kinetics, and thermodynamic properties," Malays. J. Anal. Sci., vol. 29, art. no. 1340, 2025. https://doi.org/10.17576/mjas-2025-2901-14

[50] H. J. Yu, T. T. Wang, W. Dai, L. Yu, and N. Ma, "Competitive adsorption of dye species onto biomass nanoporous carbon in single and bicomponent systems," Braz. J. Chem. Eng., vol. 35, no. 1, pp. 253-264, 20180 https://doi.org/10.1590/0104-6632.20180351s20160249

[51] A. S. Mousavi, A. Mahmoudi, S. Amiri, P. Darvishi and E. Noori, "Methylene blue removal using grape leaves waste: optimization and modeling," Appl. Water Sci., vol. 12, no. 5, art. no. 112, 2022. https://doi.org/10.1007/s13201-022-01633-z.

[52] H. N. Baharim, F. Sjahrir, M. R. Taib, N. Idris and T. A. T. Daud, "Methylene Blue Adsorption by Acid Post-Treated Low Temperature Biochar derived from Banana (Musa acuminata) Pseudostem," Sains Malaysiana, vol. 52, no. 2, pp. 547-561, 2023. http://doi.org/10.17576/jsm-2023-5202-14

[53] S. K. Dutta, M. Elias, K. M. Anis-Ul-Haque, P. K. Dhar, M. M. R. Khan and M. K. Amin, "Cost-effective and eco-friendly leaf-based bio-adsorbent for methyl blue dye adsorption: thermodynamics, kinetics, isotherms, and phytotoxicity," Res. Sq. (Preprint), 2023. https://doi.org/10.21203/rs.3.rs-2895537/v1

[54] D. K. Kumar and P. King, "Equilibrium, kinetic, and thermodynamic studies of methylene blue dye adsorption from wastewater using Manila tamarind shell copper nanoparticles as adsorbent," Nat. Environ. Pollut. Technol., vol. 24, no. 3, art. no. B4285, 2025.

[55] R. Das, A. Mukherjee, I. Sinha, K. Roy and B. K. Dutta, "Synthesis of potential bio-adsorbent from Indian Neem leaves (Azadirachta indica) and its optimization for malachite green dye removal from industrial wastes using response surface methodology: kinetics, isotherms and thermodynamic studies," Appl. Water Sci., vol. 10, no. 5, pp. 1-18, 2020. https://doi.org/10.1007/s13201-020-01186-x

[56] G. Nibret, S. Ahmad, D. Govardhana, I. Ahmad and S. Mohamed,"Removal of methylene blue dye from textile wastewater using water hyacinth activated carbon as adsorbent: Synthesis, characterisation and kinetic studies," in Proc. Int. Conf. Sustain. Comput. Sci., Technol. Manage. (SUSCOM), 2019, pp. 1959-1969. https://doi.org/10.1109/SUSCOM46429.2019.9051493

[57] Z. Ngaini, A. N, Mahmut. I. N, Adzmi. M. N, Arsat. N and Ziem. V. A,"Optimising Methylene Blue Removal Using Sago Effluent Activated Carbon: A Response Surface Methodology Study," J. Sustain. Sci. Manage., vol. 20, no. 2, pp. 346-363, 2025.

[58] Y. Miyah, A. Lahrichi, M. Idrissi, A. Khalil, and F. Zerrouq, "Adsorption of methylene blue dye from aqueous solutions onto walnut shells powder: Equilibrium and kinetic studies," Surfaces and Interfaces, vol. 11, pp. 74-81, 2018. https://doi.org/10.1016/j.surfin.2018.02.006

[59] M. A. Alkherraz, M. K. Elsherif, and H. A. Madiry, "Kinetic Isotherm and Thermodynamic Modelling of Methylene Blue Adsorption Using Green Tea-Based Biosorbents," Libyan J. Sci. (LJS), vol. 28, no. 1, pp. 41-47, 2025.

[60] D. Bhattacharya, M. Lodariya, E. Addis, D. K. Arunachalam, V. S. Mayani, and J. R Nikam, "Evaluation of the efficacy of papaya seed-based natural adsorbent for synthetic textile wastewater treatment," E3S Web Conf., vol. 603, art. no. 04018, 2025. https://doi.org/10.1051/e3sconf/202560304018

[61] Y. F. Carhuarupay-Molleda, N. M. Ccasa Barboza, S. Pastor-Mina, C. E. Duenas Valcarcel, Y. G. Palomino-Malpartida, R. Mojo-Quisani, A. Licapa Redolfo,; M. Calla-Florez, R. F. Aguilar-Salazar and Y. Flores-Ccorisapra, "A Study of Methylene Blue Adsorption by a Synergistic Adsorbent Algae (Nostoc sphaericum)/Activated Clay," Polymers, vol. 17, no. 15, art. no. 2134, 2025. https://doi.org/10.3390/polym17152134

[62] G. Mosoarca, C. Vancea, S. Popa, M. E. Radulescu-Grad, M. Dan, C. Tanasie and S. Boran, "Adsorption of Methylene Blue onto Environmentally Friendly Lignocellulosic Material Obtained from Mature Coltsfoot (Tussilago farfara) Leaves," Polymers, vol. 17, no. 11, art. no. 1549, 2025. https://doi.org/10.3390/polym17111549

[63] B. E. Onuk and B. Isik, "Adsorptive removal of toxic methylene blue and crystal violet dyes from aqueous solutions using Prunus spinosa: isotherm, kinetic, thermodynamic, and error analysis," Biomass Convers. Biorefin., pp. 1-18, 2025. https://doi.org/10.1007/s13399-024-06436-x

[64] N. Hariri, Z. Farahmandkia, E. Asgari., H. Danafar and M. M. Fazli, "A comparative study on the adsorption of methylene blue in aqueous media by activated carbon and carbon nanosheets derived from olive stones," Environ. Health Eng. Manage. J., vol. 12, art. no. 1474, 2025.

[65] H. M. Hashem, M. El-Maghrabey, and R. El-Shaheny, "Inclusive study of peanut shells derived activated carbon as an adsorbent for removal of lead and methylene blue from water," Sci. Rep., vol. 14, no. 1, art. no. 13515, 2024. https://doi.org/10.1038/s41598-024-64478-4

[66] Y. Xu, Y. Zhou, Y. Zhou, P. Wu, L. Gao and Z. Ding, "Synthesis of Magnetic Biosorbent from Bamboo Powders and Their Application for Methylene Blue Removal from Aqueous Solution: Kinetics, Isotherm, and Regeneration Studies," Molecules, vol. 30, no. 6, art. no. 1320, 2025. https://doi.org/10.3390/molecules30061320

[67] N. Albayati, M. Mohammed, H. Ahmed, and M. Kadhom, "The Potential of Gundelia Seeds Waste as an Emerging Sustainable Adsorbent for Methylene Blue-Polluted Water Treatment," Prog. Color Colorants Coat., vol. 18, no. 1, pp. 53-71, 2025. https://doi.org/10.30509/pccc.2024.167301.1278

[68] S. Kumari, S. Agarwal, M. Kumar, P. Sharma, A, Kumar, A. Hashem and M. C. Garg, "An exploration of RSM, ANN, and ANFIS models for methylene blue dye adsorption using Oryza sativa straw biomass: a comparative approach," Sci. Rep., vol. 15, no. 1, art. no. 2979, 2025. https://doi.org/10.1038/s41598-025-54602-x

مقالة بحثية

# أمتزاز الميثيلين الأزرق على أوراق القبَار اليمني (*CAPPARIS SPINOSA*): دراسات نمذجة حركية، وتماثل حراري (ايزوثرمي)، وديناميكية حرارية لمعالجة الصبغة المستدامة

عبداللطيف عبدالله مهدي سيف[1]، و أحمد عوض صالح صلاح[2،*]

[1] قسم الكيمياء، كلية التربية، جامعة عدن، اليمن
[2] قسم الاحياء والكيمياء، كلية طورالباحة الجامعية، جامعة لحج، اليمن

* الباحث الممثّل: أحمد عوض صالح صلاح؛ البريد الالكتروني: aasalehsalah.74@gmail.com

استلم في: 13 مارس 2026 / قبل في: 30 مارس 2026 / نشر في 31 مارس 2026

## المُلخّص

يشكل تصريف التدفقات السائلة الملوثة بالأصباغ الناتجة عن الأنشطة الصناعية تهديداً خطيراً للبيئات المائية نظراً لسميتها، وثباتها، وتأثيرها الجمالي السلبي. في هذه الدراسة، تم تقييم أوراق القبَار المجففة (CPL) كممتز حيوي منخفض التكلفة وصديق للبيئة لإزالة صبغة الميثيلين الأزرق (MB) من المحاليل المائية .أُجريت تجارب الامتزاز بنظام الدفعات لاستقصاء تأثيرات كل من زمن التلامس، جرعة المادة المازة، والتركيز الأولي للصبغة، والرقم الهيدروجيني للمحلول، ودرجة الحرارة. كما تم تحديد المجموعات الوظيفية السطحية لأوراق القبَار باستخدام مطيافية الأشعة تحت الحمراء بتحويل فورييه. (FTIR) وتم تحليل توازن الامتزاز، والسلوك الحركي، و الديناميكية الحرارية باستخدام نماذج "لانجمويير" و"فروينديليش" التماثل الحراري(الايزوثرمي)، ونماذج الحركية من الرتبة الأولى الكاذبة والرتبة الثانية الكاذبة، والمعاملات الديناميكية الحرارية: التغير في الطاقة ($\Delta G°$) ، والتغير في الانثالبي ($\Delta H°$)، والتغير في الانتروبي ($\Delta S°$) على التوالي. وقد خلصت الدراسة إلى النتائج التالية: تم تحديد عملية الامتزاز عند الرقم الهيدروجيني 8 مع ملاحظة أعلى كفاءة إزالة عند الرقم الهيدروجين12. وحقق زمن التلامس لمدة 40 دقيقة بمعدل إزالة 91.58%، وبسعة امتزاز بلغت 1.99 مجم/جم. وقد تم تسجيل أعلى سعة امتزاز بواقع 12.469 مجم/جم عند تركيز صبغة 20 جم/لتر، وجرعة 0.5 جم، وبكفاءة إزالة مثالية وصلت إلى99.95%. أظهرت بيانات التوازن أفضل مطابقة لنموذج "لانجمويير"($R^2$=0.9997) من نموذج فروينديليش ($R^2$=0.894) والتي اثبتت ان عملية الامتزاز تم على طبقة احادية ذات سطح متجانس ومعامل الفصل 0.4332 ($R_L$) والذي اثبت بأن امتزاز الميثيلين الأزرق على أوراق القبار عملية مناسبة ، بينما اتبعت البيانات الحركية نموذج الرتبة الثانية الكاذبة($R^2$= 0.9995) من نموذج الرتبة الاولى الكاذبة ($R^2$=0.9296) وقد اقتربت قيمة $q_{e,cal}$ المحسوبة (2.07 mg/g) مع قيمة $q_{e,exp}$ (1.99 mg/g). حيث أكد التحليل الديناميكي للتغير في الانتروبي 80.041kJ/mol ($\Delta H°$) أن امتزاز الميثيلين الأزرق على أوراق القبارهو عملية ماصة للحرارة، والتغير في الطاقة ($\Delta G°$) (-6.687, -9.597, -12.508, and -15.418kJ/mol) بتلقائية عملية الامتزاز. تُثبت هذه النتائج أن أوراق القبَار هي ممتز مستدام وواعد لمعالجة مياه الصرف الصحي الملوثة بالأصباغ.

**الكلمات المفتاحية:** القبَار (*Capparis spinosa*)؛ الميثيلين الأزرق؛ الممتز الحيوي؛ التوازن؛ متماثلات حرارة الامتزاز؛ الحركية؛ الديناميكا الحرارية؛ معالجة مياه الصرف الصحي.

## How to cite this article:

A. A. M. Saif, and A. A. S. Salah, "ADSORPTION OF METHYLENE BLUE ONTO YEMENI CAPPARIS SPINOSA LEAVES: KINETIC, ISOTHERM, AND THERMODYNAMIC MODELING STUDIES FOR SUSTAINABLE DYE REMEDIATION", *Electron. J. Univ. Aden Basic Appl. Sci.*, vol. 7, no. 1, pp. 135-150, Mar. 2026. DOI: https://doi.org/10.47372/ejua-ba.2026.1.522